Experimental Study on Velocity Profiles with Different Roughness Elements in a Flume

Xie-Kang WANG[1], Chen YE[1], Bing-Jie WANG[1], and Xu-Feng YAN[2]

[1]State Key Laboratory of Hydraulics and Mountain River Engineering,
Sichuan University, Chengdu, China;
e-mail: wangxiekang@scu.edu.cn (corresponding author)

[2]Department of Civil and Environmental Engineering, Hong Kong Polytechnic
University, Hong Kong, China; e-mail: xufeng.yan@connect.polyu.hk

A b s t r a c t

The classical log law for velocity profile is applied to engineering practice. Field observations indicate that the composition of the bed materials obviously influences the shape of vertical velocity distribution. To clearly understand the roughness effect, six types of materials were laid separately at various depths for the investigation of the effects of roughness elements on the vertical velocity distribution. A down-looking 3D acoustic Doppler velocimeter was used to measure the velocity profiles. The experimental results showed that the curve characteristics of velocity profiles are strongly dependent on the roughness scale and related flow parameters. If d/R, Fr, and Re are larger than 0.15, 0.47, and 60 000, respectively, the velocity distribution may resemble an S-shape profile. The inflexion position Z_*/H for a given S-shape profile was empirically deduced as $Z_*/H = -0.4481 d/R + 0.3225$. Otherwise, the velocity profile agrees well with the logarithmic law. The findings of this study are useful in engineering practice (*i.e.*, depth-averaged velocity and flow rate estimate).

Key words: velocity profiles, acoustic Doppler velocimeter, roughness elements, logarithmic law, S-shape curve.

1. INTRODUCTION

Most flow structure studies in open channel focus mainly on the velocity profile since it has been often used to examine the local effects due to roughness elements on the flow field and flow resistances (Nowell and Church 1979, Raupach 1981, Dong and Ding 1990, Dong *et al.* 1992, Robert *et al.* 1992, Wohl and Ikeda 1998, Tachie *et al.* 2000, Ferro 2003a, b). The classical logarithmic velocity profile is employed as the boundary condition linking the boundary node and the first calculated internal node, so that the large computational time consumption can be reduced in modeling the boundary layer (Lin and Li 2002, Knopp *et al.* 2006). The velocity profile indicates the mass transport distribution and the momentum transfer.

Back to the last century, Kuelegan (1938) proposed the velocity profile fitting the log-law along the entire depth. With the advanced experimental investigation and theoretical analysis, the velocity distribution often varied with the bed roughness scales. In the 1980s, the previous studies (Zippe and Graf 1983, Nezu and Rodi 1986) showed that the log law could only be established in the region of near-wall, and the logarithmic formula should be extended with a wake function for the whole depth (Coles 1956, Kirkgöz 1989, Kirkgöz and Ardiçlioğlu 1997, Liu *et al.* 2005). Cardoso *et al.* (1989), however, pointed out that wake function might be affected by secondary flows, upstream flows, and so forth. Wang *et al.* (1998), comparing the developing flows within the boundary layer, thought that the wake function was essentially an empirical processing of measured data, and thus no universal wake function exists to cover all situations. Papanicolaou *et al.* (2012) successfully introduced the velocity defect law to describe the velocity distribution around the boulder within the array. Many research studies also document the characteristics of velocity profile regarding the effects of different roughness scales. Bathurst *et al.* (1981) defined roughness as small a scale as $h/d_{50} > 7.5$ or $h/d_{84} > 4.0$, (d_{50}, the particles for which 50% are finer; d_{84}, the particles for which 84% are finer); however, Bray (1988) believed that the quantity of the relative depth for small scale roughness is $h/d_{50} > 20$. Dong and Ding (1990) and Dong *et al.* (1992) studied the influence of boundary roughness on flow characteristics by changing the value of h/k_s. He suggested that the velocity profile is able to be fitted just by the logarithmic formula if $h/k_s < 2.0$ (k_s is 10 mm, the maximum diameter of bed materials), while the wake function should be introduced if $h/k_s \geq 5.0$. He and Wang (2004) also pointed out that the velocity profile on rough beds cannot be described with a single logarithmic formula. Jiménez (2004) believed that for the logarithmic layer to occur the relative depth (flow depth to the roughness height ratio) should exceed at least 40. On the basis of the flume experiments using pingpong balls instead of sand grains, Yang and Yang (2005) showed

that the velocity profile only complies with the log law when $h/k_s > 1.9$ (k_s is 4.0 cm, the diameter of pingpong ball).

The log law for fitting the boundary flow velocity distribution is classical due to its simple description, the explanation of mechanism, and universality for the boundary conditions. The velocity profile, however, does not frequently satisfy the log law in realistic rivers, in particular steep mountain rivers with high flow condition and large-scale roughness (*i.e.*, gravel and cobble) (Biron *et al*. 1998, Wohl and Thompson 2000). Katul *et al*. (2002) believed that when the ratio of the water depth and roughness scale is small (< 10), the boundary layer theory becomes invalid to estimate the flow discharge and flow resistance. Byrd *et al*. (2000) presented that only a small proportion (10%) among all field measured velocity distributions could be described by the logarithmic profile, while the majority was attributed to other profiles, including S-shape profile, irregular profile, and linear profile. Schmeeckle and Nelson (2003) reported that the wake effect induced by roughness elements plays significant role in formation of S-shape velocity profile. Studies by Shvidchenko and Pender (2001) show that the drag force induced by the large-scale roughness elements significantly negatively contributes to the velocity distribution within the lower layer of the water depth. Byrd *et al*. (2000), employing the scaling analysis of the momentum and kinetic energy equations, showed that terms usually neglected in cases with small-scale roughness became significant in very rough mountain rivers. This change was the rooted reason for occurrence of the non-logarithmic velocity profiles such as S-shape profiles. Similar S-shape velocity profiles can be extensively identified regarding the flow through canopies, including terrain canopies and aquatic canopies (Raupach *et al*. 1996, Nepf and Ghisalberti 2008) and atmospheric flow over urban roughness (Kastner-Klein and Rotach 2004, Coceal *et al*. 2006). The S-shape velocity profile also frequently coincides with the bed-forms such as large-scale dunes due to bed-load transport. The above-mentioned studies all indicate that the velocity profile is highly correlated to the roughness scale. The logarithmic profile corresponds with small-scale roughness, while the S-shape profile with large-scale roughness (Franca 2005).

In order to explore the cause of occurrence of the irregular velocity profile (*i.e.*, S-shape profile), the turbulence structure near the bed with large-scale roughness (*i.e.*, gravels and cobbles) were examined recently. Roy *et al*. (2004) with the field investigation results showed that the large-scale turbulent flow structures over the gravel bed developed within the entire water depth, which led to the disappearance of the boundary layer. Hardy *et al*. (2009) demonstrated that the turbulent coherent structure was triggered by the flow wake flapping around the roughness (gravels), and more well-organized with the increase in the Reynolds number. Further, other more re-

lated studies can be found to understand the flow turbulent behavior near the rough bed (Buffin-Bélanger and Roy 2005, Legleiter *et al.* 2007, Singh *et al.* 2010). Because of the complicated flow structure characteristics induced by the rough boundary, researchers (Nikora *et al.* 2007, Aberle *et al.* 2008, Stoesser and Nikora 2008) have recently employed the time-averaging concept to spatially average the Reynolds averaged Navier–Stokes equations, obtaining a new term referred to as form-induced stress analogous to Reynolds stress. With the simplification, it is found that the form-induced stress and associated turbulent kinetic energy might be the source to result in the irregular velocity profile (Cooper and Tait 2008, Mignot *et al.* 2008, 2009).

The categories of velocity profiles are conventionally divided into log-law and log-wake-law types within the open channel. Based on the experimental studies (Marchand *et al.* 1984, Bathurst 1988, Ferro and Baiamonte 1994), the velocity profile, however, may be described as an S-shaped type with near-surface velocities significantly greater than near-bed velocities over large scale roughness with the depth/sediment ratio (h/d_{84}) ranging from 1.0 to 4.0. At the same time, two conditions for the development of an S-shaped profile were given by Bathurst (1988). These were (i) channel slopes above 1.0%, the depth sediment ratio h/d_{84} from 1.0 to 4.0, and (ii) particular bed materials with non-uniform condition to allow the development of the lower zone flow. Ferro (2003a) developed a mathematical equation with four parameters to reproduce the measured S-shaped velocity profile in a laboratory flume. Ferguson (2007) agreed that the log law becomes invalid as the ratio of the water depth and the roughness layer thickness decrease below 4.0, while the S-shape profile is applicable.

Bathurst (1985) pointed out the depth/sediment ratio (h/d_{84}) has to vary from 1.0 to 4.0 to form an S-shaped velocity profile, and the upper limit of h/d_{84} defines the point at which the projection of bed material into the flow becomes relatively insignificant. Ferro (2003a) agreed on Bathurst's statement, while further modified the depth sediment ratio h/d_{84} ranging from 1.17 to 12.12 according to experimental data. Afzalimehr *et al.* (2011) also achieved a similar result of S-shape velocity profile within the cobble-bed rivers but not for all cases. The range of the relative submergence is suggested as $2.0 < h/d_{84} < 4$. In this present study, a filed surveys firstly verified that the different roughness element affected changes of vertical velocity profile in mountain river with wide size distribution sediment, and then, the effects of relative roughness ratio $4.9 < h/k_s < +\infty$ and $1.0 < B/h < 4.0$ on velocity profiles are further explored in the flume experiment. Also discussed are the two other questions: (i) whether or not there exists an S-shaped profile on a artificial bed with a flat slope arrangement, and (ii) how to determine the logarithmic or S-shape curves according the flow and

boundary conditions; in other words, how to achieve the inflexion position for the given S-shape curve.

2.   METHODOLOGY

2.1 Experimental setup

Most field surveys show that there is a non-uniform sediment on the bed materials in mountain river, the patterns of sediment sorting in this wide size distribution sediment commonly result from the segregation of particles with the interaction between flow and sediment, and then the uniform sediment region often occurs in some local small unit area. In order to choose the diameter of experimental sediment in the flume, we investigated the characteristics of bed materials at the intersection between the Baisha River and Mingjian River at Dujiangyan irrigation system in Chengdu, China. Physically, the typical vertical velocity distribution and the flow rate were measured using the FlowTracker Handheld acoustic Doppler velocimeter (ADV) manufactured by SonTek/YSI. Figure 1 presents the monitoring photos and the related sediment characteristics on the river bed. Figure 1a indicates that different uniform sediment groups were distributed on the river bed. Figure 2a shows the vertical water depth distribution at Baisha River. The mean flow velocity was estimated at the 0.6 local water depth (see Fig. 2b). The flow rate was calculated by the single-point method in hydrological analysis, as a consequence of 0.512 m³/s of the flow discharge with respect to Baisha River. The detailed vertical velocity profile in Fig. 2c has been monitored at four typical positions (*i.e.*, a distance of 1.4, 1.8, 2.8, and 3.8 m, respectively), showing that in the shape of velocity profile there obviously exist some differences; this result may affect the precision of flow rate calculation assuming the logarithmic law of velocity profile. The velocity data at regions from the river bed to the 0.2 dimensionless water depth, however, cannot be obtained because of the limitation of the FlowTracker Handheld ADV system monitoring blindness zone. The flume experiment would be designed and completed to systematically explore the influence of bed roughness on the velocity distribution.

The experiments were carried out in a flume with size of 0.60 m (width) × 0.60 m (depth) × 13.5 m (length) and a flat slope, located in the State Key Laboratory of Hydraulics and Mountain River at Sichuan University (China). The test zone shown in Fig. 3 is 4.0 m long, where two typical cross-sections with intervals of 20 cm among sections were selected in the middle reach within the flume. The velocity profile was uniformly measured along five verticals distributed at each cross-section, *i.e.*, line 1#, line 2#, line 3#, line 4#, and line 5#, at positions of 0.10, 0.20, 0.30, 0.40, and 0.50 m, respectively. The measurement interval distance is 0.5 cm within regions of
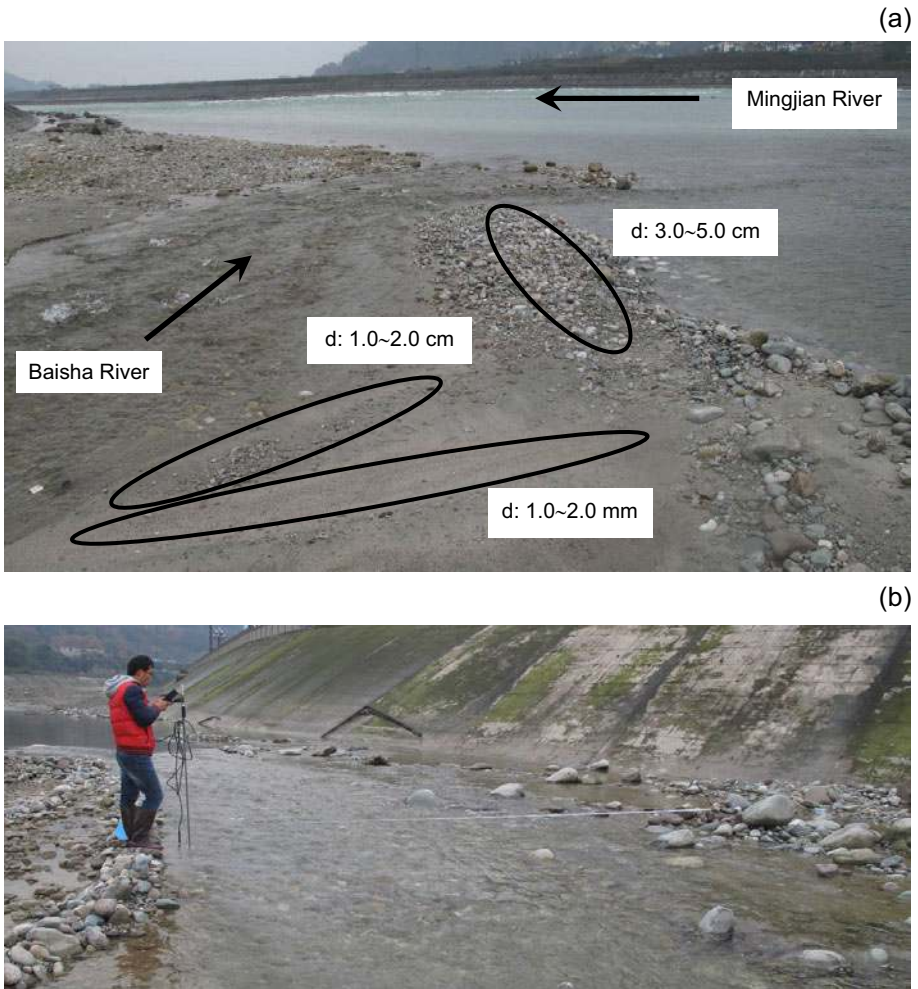
(a)

(b)

Fig. 1. Field observation photos showing the diameters of bed materials and flow velocity: (a) the diameter characteristics of bed materials at Baisha River in river confluence, and (b) observational section of vertical velocity profile and flow rate at Baisha River.

2.0 cm above the bottom, and 1.0 cm within outer regions in order to obtain detailed velocity field in each vertical monitoring line. Based on findings of previous studies which investigated velocity profiles, the uniform sands were used in this study to dispose of the effects of k_s on the conditions of roughness scales because of the uncertainty of roughness height k_s for the different selection criteria, *i.e.*, $k_s = d_{65}$, d_{75}, d_{84} or d_{90} (Einstein and El-Samni 1949, Lane and Carlson 1953, Bathurst *et al.* 1981, Meyer-Peter and Müller 1948).
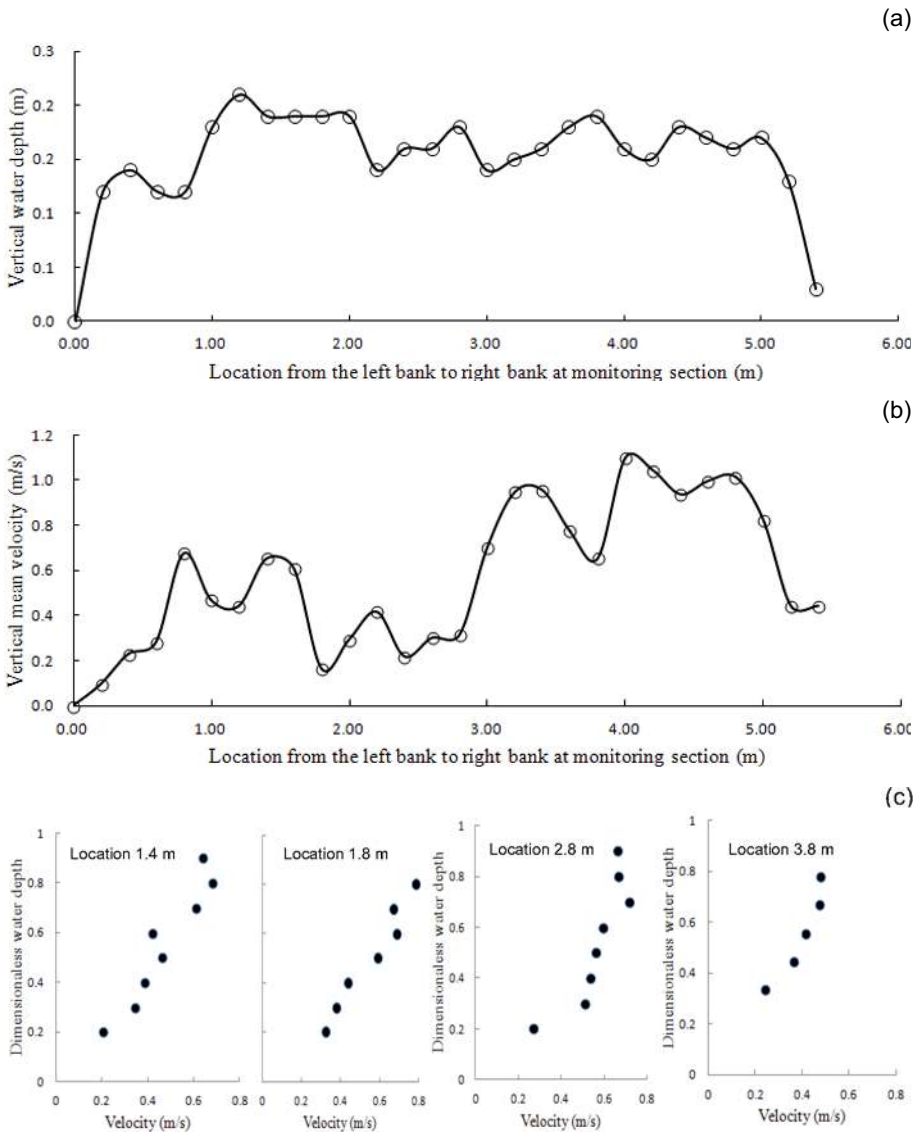
(a)

(b)

(c)

Fig. 2. The flow characteristics at flow rate monitoring section in Baisha River: (a) the vertical water depth distribution at flow rate monitoring section, (b) the vertical velocity distribution at 0.6 h position in flow rate monitoring section, and (c) the vertical velocity profile at typical locations in flow rate monitoring section.

Beds with five types of sediment roughness and a smooth bed were set up, the diameter of the uniform sands ranging from 2.0 to 40 mm, as shown in Figs. 4 and 5.
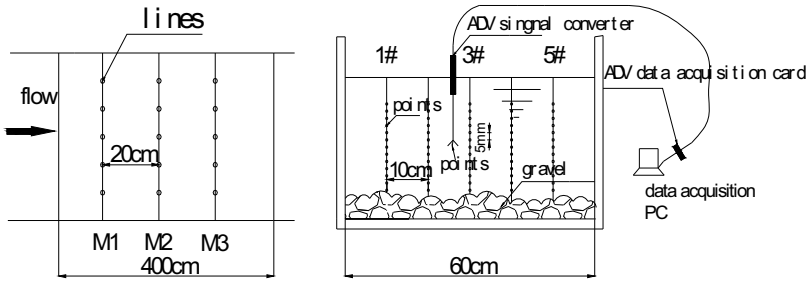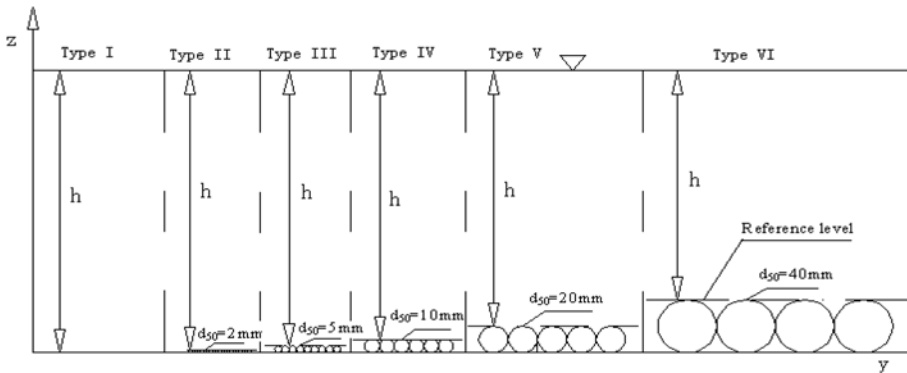
Fig. 3. Arrangement of measurements.

Fig. 4. Schemes of bed types in experiments.

Fig. 5. Photos of bed types used in experiments.

Table 1

Parameters of experimental runs

Bed shape	Run	Section	h [cm]	B/h	R [m]	Q [l s^{-1}]	h/k_s	V [ms^{-1}]	d/R	Fr	u^* [cms^{-1}]	Re	Mean velocity shape
Type I	1	1#	50.2	1.2	0.19	83.3	+∞	0.28	0.00	0.12	1.30	41915	Log
		2#	50.1	1.2	0.19	83.3	+∞	0.28	0.00	0.12	1.28	41967	Log
	2	2#	29.3	2.0	0.15	84.2	+∞	0.48	0.00	0.28	2.11	57300	Log
		6#	29.3	2.0	0.15	84.2	+∞	0.48	0.00	0.28	2.20	57300	Log
Type II	3	1#	42.0	1.4	0.18	74.9	210	0.30	0.01	0.15	1.60	41981	Log
		2#	42.0	1.4	0.18	74.9	210	0.30	0.01	0.15	1.48	41981	Log
Type III	4	1#	37.0	1.6	0.17	84.9	74.0	0.38	0.03	0.20	2.30	51137	Log
		2#	37.0	1.6	0.17	84.9	74.0	0.38	0.03	0.20	2.11	51137	Log
	5	2#	24.5	2.4	0.13	78.1	49.0	0.53	0.04	0.34	2.95	57830	Log
		4#	24.7	2.4	0.14	78.1	49.4	0.53	0.04	0.34	2.65	57619	Log
Type IV	6	1#	30.7	2.0	0.15	71.7	30.7	0.39	0.07	0.22	3.09	47668	Log
		2#	30.7	2.0	0.15	71.7	30.7	0.39	0.07	0.22	2.88	47668	Log
	7	2#	17.4	3.4	0.11	71.7	17.4	0.69	0.09	0.53	3.51	61044	S
		4#	18.1	3.3	0.11	71.7	18.1	0.66	0.09	0.50	3.42	60155	S
	8	2#	16.7	3.6	0.11	77.6	16.7	0.77	0.09	0.61	4.04	67057	S
		3#	17.1	3.5	0.11	77.6	17.1	0.76	0.09	0.58	4.26	66487	S
	9	2#	18.0	3.3	0.11	76.9	18.0	0.71	0.09	0.54	4.71	64652	S
		4#	18.0	3.3	0.11	76.9	18.0	0.71	0.09	0.54	4.72	64652	S
Type V	10	2#	31.0	1.9	0.15	61.2	15.5	0.33	0.13	0.19	2.79	40487	Log
		4#	31.0	1.9	0.15	61.2	15.5	0.33	0.13	0.19	2.96	40487	Log
	11	2#	28.6	2.1	0.15	72.3	14.3	0.42	0.14	0.25	4.12	49790	Log
		6#	29.0	2.1	0.15	72.3	14.5	0.42	0.14	0.25	4.12	49452	Log
	12	2#	18.4	3.3	0.11	76.8	9.2	0.70	0.18	0.52	5.51	64035	S
		4#	19.5	3.1	0.12	76.8	9.8	0.66	0.17	0.47	5.40	62612	S
	13	2#	17.9	3.4	0.11	77.2	9.0	0.72	0.18	0.54	6.41	65040	S
		3#	17.2	3.5	0.11	77.2	8.6	0.75	0.18	0.58	6.20	66005	S
Type VI	14	1#	22.8	2.6	0.13	98.3	5.7	0.72	0.31	0.48	9.24	75131	S
		2#	22.1	2.7	0.13	98.3	5.5	0.74	0.31	0.50	9.14	76140	S
	15	1#	20.2	3.0	0.12	101	5.1	0.83	0.33	0.59	9.75	81193	S
		2#	19.7	3.0	0.12	101	4.9	0.85	0.34	0.61	9.66	82009	S

Explanations: Type I – smooth bed; Type II – uniform sand with 2 mm diameter; Type III – uniform sand with 5 mm diameter; Type IV – uniform sand with 10 mm diameter; Type V – uniform sand with 20 mm diameter; and Type VI – uniform sand with 40 mm diameter.

In this experiment, the flow velocities were measured by a down-looking 3D acoustic Doppler velocimeter (ADV) probe with the standard 16-MHz, which is manufactured by SonTek Inc. The research was done under the fol-

lowing conditions: (i) the sampling volume by ADV was small (*i.e.*, 0.125 cm^3), (ii) the sampling location was situated 5.0 cm below the sensor head, and (iii) the instrument sensed the distance between the bottom of the measuring volume and the bed surface with a high degree of accuracy (±1 mm). The above enables precise determination of the position of each velocity measurement (Bergeron and Abrahams 1992), and acquisition of a high-resolution record of the vertical velocity variation with minimal profile disturbance due to the presence of the probe.

2.2 Analysis of velocity profiles

The flow velocity measurements were carried out under different discharges, and related hydraulic variations were calculated as shown in Table 1, *i.e.*, values of the width/depth ratio B/h and of depth/roughness height ratio h/k_s, (k_s is the median diameter of uniform sands), hydraulic radius R, relative roughness d/R, average velocity $V = Q/(B h)$, the Froude number Fr = $Q/(g^{1/2} B h^{3/2})$, Reynolds number (Re = VR/v; v is water kinematic viscosity with magnitude of 0.01239 cm^2/s with water temperature 12° in this experiment).

2.3 Vertical velocity profiles

Figure 6 shows that the longitudinal velocities at the same cross-section for an individual run nearly collapse onto the logarithmic profile despite different transverse distances against the wall. This indicates the limited side boundary effect on the velocity distribution so that the measurements are reliable. Figure 7 shows that an alternative S-shape velocity profile occurs for different bed roughness and flow conditions. Traveling along this profile, the velocity at lower layers is significantly resisted, with an inflexion point at the upper layer. This phenomenon is consistent with the descriptions based on previous studies (Marchand *et al.* 1984, Liu *et al.* 2005, Afzalimehr *et al.*
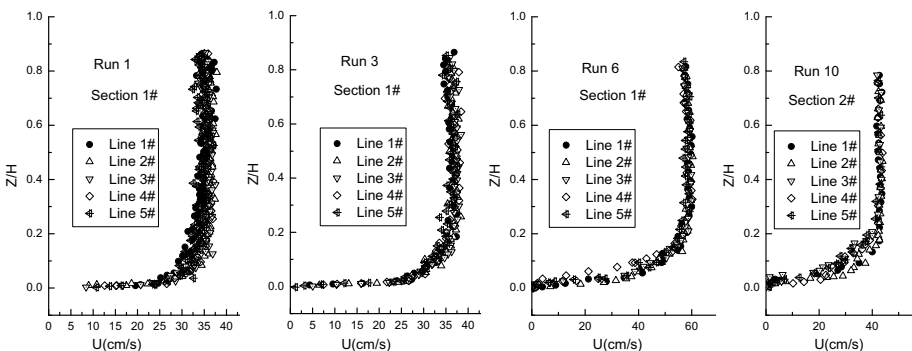

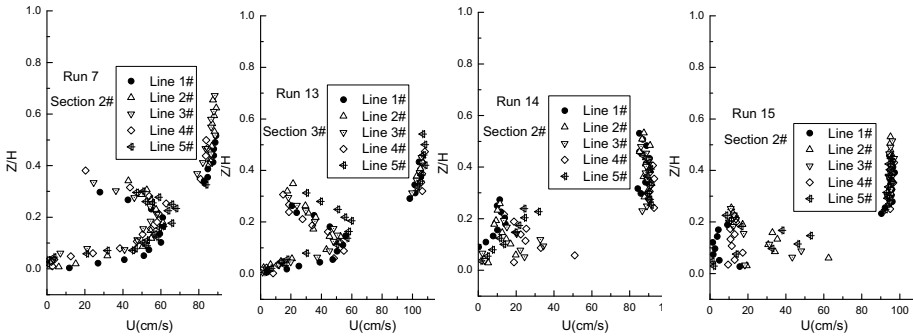Fig. 6. Logarithmic curves of vertical velocity profiles.

Fig. 7. The S-shape curves of vertical velocity profiles.

2011). However, the previous studies, besides the scale of roughness, did not adopt the flow condition characterized by the Froude number, Fr, as a factor to determine the pattern of velocity profiles. The influence of the Froude number, Fr, on the velocity profile will be analyzed and discussed in the subsequent part of the article.

2.4 Shear velocity estimation

The analysis of velocity profiles frequently employs the shear velocity to represent the dimension of velocity to obtain the formula of velocity description. However, the shear velocity is a somewhat artificially created variable, able to be calculated from the bed shear stress. Rowiński *et al.* (2005) discussed 10 methods including the gravity method, logarithmic profile method, near-bed Reynolds-stress method, turbulent kinetic energy method, Prandtl-based method, *etc.* Those authors pointed out the variability of different methods which can be applied to estimate bed shear stress. With the measurement of high-frequency velocity fluctuations, the measured turbulence may be used in the determination of the shear velocity. For example, Laser Doppler Anemometers (LDA) or ADV provides information on the instantaneous 3D velocities within a small sampling volume that makes it possible to obtain various turbulence parameters (*e.g.*, Nikora and Goring 1998). Conventionally, the most frequently used method to calculate the shear frictional velocity is fitting the log-law velocity profile. However, the velocity profile does not satisfy the log law any longer when large-scale roughness exists at the bottom, as mentioned above. Comparably, the kinetic energy method is very straightforward to calculate the shear velocity once the distribution of the turbulent kinetic energy is obtained by measurements. Wang *et al.* (2007) stated that the 3-D turbulence kinetic energy method (*i.e.*, Kim *et al.* 2000, Biron *et al.* 2004) is the correct method to determine the shear velocity on a rough river bed. This method, therefore, is also used in this study. The method is based on the formula $\tau_0 = \rho U_*^2 = 0.5 C \rho (\overline{u'^2} + \overline{v'^2} + \overline{w'^2})$, where C

is assumed to be equal to 0.19. This method has been proved to be applicable in gravel beds (Schindler and Robert 2005).The shear velocities for each run are listed in Table 1.

Figure 8 presents mean velocity profiles with normalization of the shear velocity at the selected cross-section for each run, in which the mean velocity has been calculated by averaging velocities with respect to five vertical lines and normalized with the shear velocity, as shown in Table 1. It is to be noted from Fig. 8 that the velocity increases and fits log law through the increasing water depth in Runs 1-6 and 10-11. Further, there occurred an inflexion located within the range of 0.15~0.30 Z/H (H is the averaged depth) away from the bed for the Runs 7-9 and 12-15. As a result, the mean velocity collapses into an S-shape curve. Comparing Run 6 with Run 7, the mean velocity profiles are respectively characterized by logarithmic and S-shape curves with the same discharge of $71.7 \, 1 \, s^{-1}$ and bed materials with uniform sands of 10 mm diameter and but different flow depths. Generally speaking, the flow structures are strongly dependant on flow conditions (*i.e.*, Froude number, Fr; Reynolds number, Re) and boundary conditions (*i.e.*, hydraulic radius, relative roughness d/R, the value of width/depth ratio B/h).

To further reveal the relationships among the bottom roughness, d/R, flow conditions, Fr, and Reynolds number, Re, on the patterns of velocity profile, the relationship between the profile pattern and the influential factors is plotted in Fig. 9. The roughness scale d/R is set as the *x*-axis and the Froude number, Fr, and Reynolds number, Re, as the *y*-axis. As shown in the diagram, the S-shape velocity profile coincides with the relatively large-scale roughness, which has the roughness height of 10 mm above. With respect to these situations, the Froude number has larger value; when Fr > 0.47, the S-shape velocity profile could be formed in this study. In addition, the character of flow turbulence (Reynolds number) indicates that when Re > 60 000, the S-shape curve occurs in these runs.

As discussed above, the logarithmic velocity profile is not satisfactory for description of the velocity over the very rough bed with the high Froude number and Reynolds number. The S-shape velocity profile may be an alternative distribution. Generally speaking, the wall function method that employs the log law or power law for velocity connection between the boundary node and the first internal node is very powerful to in the numerical simulation of turbulent flows. However, within the situation that the S-shape velocity may occur, it is more appropriate to use an S-shape velocity profile to set the wall function. The hyperbolic tangent function as proposed by Katul *et al.* (2002) can be used to describe the S-shape velocity profile which inherently has an inflexion point on the profile. It is clearly noted that the inflexion position varies with the roughness scale and flow condition. Determination of the inflexion position regarding different boundary and flow
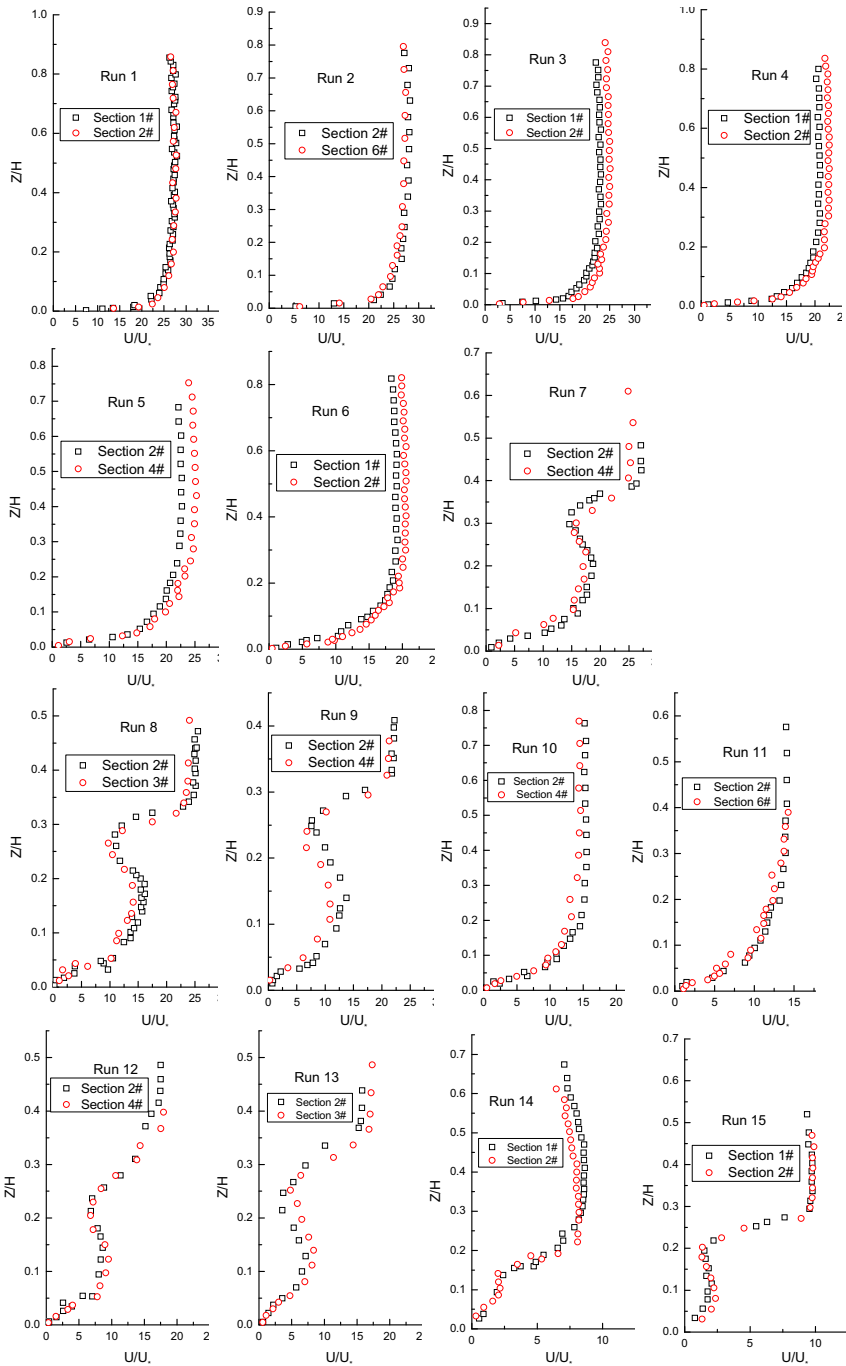
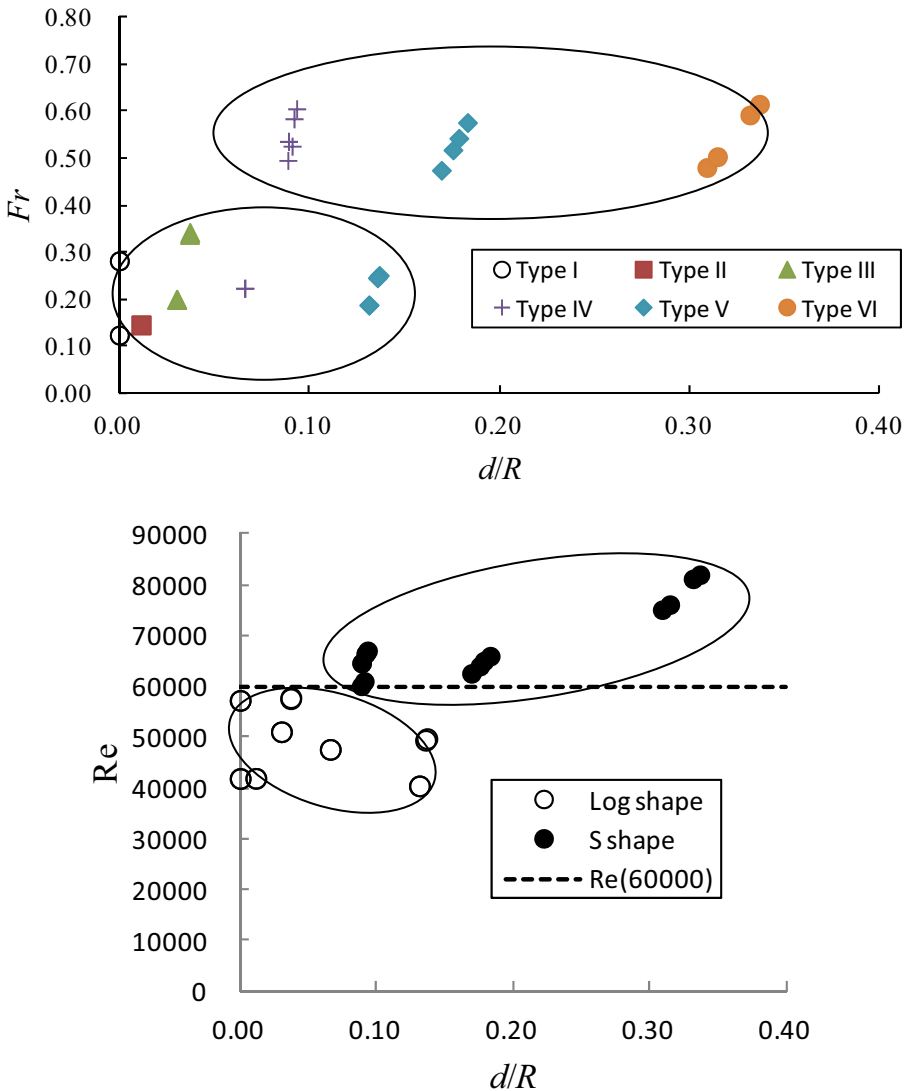Fig. 8. Mean velocity profiles at selected cross-sections in each run.

Fig. 9. The relationship between the patterns of velocity profile and related influential factors.

flow configurations is very important in engineering practice. Based on the present experiment, the inflexion position of the S-shape velocity profiles may be obtained. The linear regression equation $Z_*/H = -0.4481d/R + 0.3225$ with high correlation coefficient $r^2 = 0.8206$ can be easily obtained, as shown in Fig. 10. This equation indicates that the inflexion position decreases as the roughness scale increases.
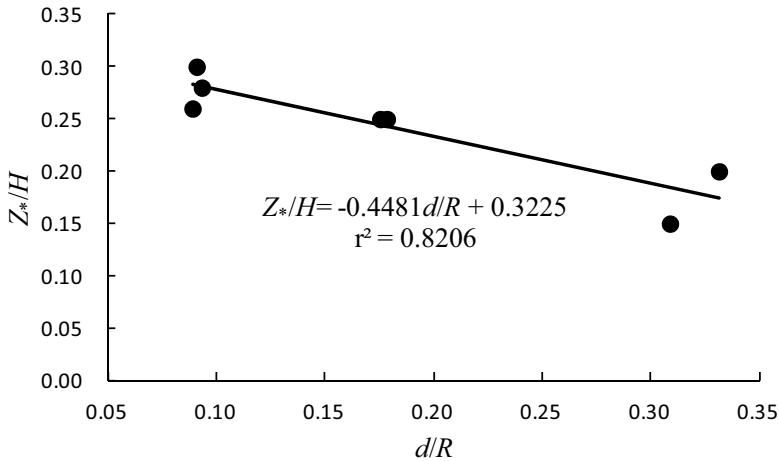
Fig. 10. The relationship between inflexion position Z_*/H and d/R.

3. CONCLUSIONS

The main aim of this study, based on previous studies, is to discuss the influence of the flow and boundary conditions (*i.e.*, $1.0 < B/h < 4.0$ and $4.9 < h/k_s < +\infty$) on the pattern of the velocity profile, namely logarithmic and S-shaped curves. Firstly, the field observations of sediment characteristics and vertical velocity profile in a mountain river with bed of different roughness have been carried out, and then the bed materials of uniform sands in flume experiment were used to observe the effects of roughness height k_s on the roughness scale, and to examine conditions of bed materials and bed slope in the development of such S-shaped velocity profiles as proposed by Bathurst (1988). The experimental results present the S-shaped velocity distribution that may occur when the uniform sands and flat slope are given. Secondly, the conditions of flow and boundary for different velocity profile types were also obtained. Based on the results of the present study it is shown that the patterns of the velocity profile are dependent on both the bottom roughness scale and the flow conditions, as compared with previous studies in which the former parameter was regarded as the only influential factor. The velocity profile may resemble an S-shape curve when the roughness height/hydraulic radius ratio $d/R > 0.15$, Froude number $Fr > 0.47$, and $Re > 60\,000$. Considering that the S-shape velocity profile occurs instead of the classical logarithmic profile for cases with large bottom roughness scale and fast velocity flows (relatively high Fr and Re), it is very important to localize the inflexion position on the S-shape profile for practical applications, such as the boundary specification in the numerical modeling. It is identified that the inflexion position Z_*/H for a given S-shape curve

could be empirically deduced as $Z_*/H = -0.4481d/R + 0.3225$ with high correlation coefficient $r^2 = 0.8206$. The velocity profile, otherwise, agrees with the logarithmic law. Finally, the regression formula of velocity profiles is not further explored because it has been satisfactorily examined in most previous studies on logarithmic velocity distributions (Keulegan 1938, Coles 1956, Marchand *et al.* 1984, Bathurst 1988, Kirkgöz 1989, Dong and Ding 1990, Dong *et al.* 1992, Ferro and Baiamonte 1994, Kirkgöz and Ardiçlioğlu 1997, Ferro 2003a, Liu *et al.* 2005, Yang and Yang 2005).

Nomenclature

ADV	– acoustic Doppler velocimeter
B	– the main flume width
C	– the empirical coefficient
d	– the sediment diameter
d_{50}	– the particles for which 50% are finer
d_{65}	– the particles for which 65% are finer
d_{75}	– the particles for which 75% are finer
d_{84}	– the particles for which 84% are finer
d_{90}	– the particles for which 90% are finer
Fr	– Froude number
g	– the gravity acceleration
h	– the water depth
H	– the average water depth
i#	– the measurement vertical number
k_s	– the bed roughness
LDA	– laser Doppler anemometers
M_i	– the *i*-th measurement cross-section in the flume experiment
Q	– the discharge [m^3/s]
R	– the hydraulic radius
Re	– Reynolds number
$u*$	– the bottom shear velocity
u', v', w'	– the fluctuating velocity in *x*-, *y*-, and *z*-directions
v	– the mean velocity
Z	– the measuring position of vertical velocity above smooth bed

$Z*$ – the inflexion position of velocity profile above smooth bed

ρ – the water density

τ_0 – the bottom shear friction

R e f e r e n c e s

Aberle, J., K. Koll, and A. Dittrich (2008), Form induced stresses over rough gravel-beds, *Acta Geophys.* **56**, 3, 584-600, DOI: 10.2478/s11600-008-0018-x.

Afzalimehr, H., J. Gallichand, J. Sui, and E. Bagheri (2011), Field investigation on friction factor in mountainous cobble-bed and boulder-bed rivers, *Int. J. Sediment Res.* **26**, 2, 210-221, DOI: 10.1016/S1001-6279(11)60087-5.

Bathurst, J.C. (1985), Flow resistance estimation in mountain rivers, *J. Hydraul. Eng. ASCE* **111**, 4, 625-643, DOI: 10.1061/(ASCE)0733-9429(1985)111:4 (625).

Bathurst, J.C. (1988), Velocity profile in high-gradient, boulder-bed channels. **In:** *Proc. Int. Conference on Fluvial Hydraulics, IAHR, 30 May – 3 June 1988, Budapest, Hungary*, 29-34.

Bathurst, J.C., D.B. Simons, and R.M. Li (1981), Resistance equation for large-scale roughness, *J. Hydraul. Div. ASCE* **107**, 12, 1593-1613.

Bergeron, N.E., and A.D. Abrahams (1992), Estimating shear velocity and roughness length from velocity profiles, *Water Resour. Res.* **28**, 8, 2155-2158, DOI: 10.1029/92WR00897.

Biron, P.M., S.N. Lane, A.G. Roy, K.F. Bradbrook, and K.S. Richards (1998), Sensitivity of bed shear stress estimated from vertical velocity profiles: The problem of sampling resolution, *Earth Surf. Process. Land.* **23**, 2, 133-139, DOI: 10.1002/(SICI)1096-9837(199802)23:2<133::AID-ESP824>3.0.CO; 2-N.

Biron, P.M., C. Robson, M.F. Lapointe, and S.J. Gaskin (2004), Comparing different methods of bed shear stress estimates in simple and complex flow fields, *Earth Surf. Process. Land.* **29**, 11, 1403-1415, DOI: 10.1002/esp. 1111.

Bray, D.I. (1988), A review of flow resistance in gravel bed rivers. **In:** C. Colosimo and M. Veltri (eds.), *Leggi morfologiche e loro verifica di campo*, BIOS, 23-57.

Buffin-Bélanger, T., and A.G. Roy (2005), 1 min in the life of a river: Selecting the optimal record length for the measurement of turbulence in fluvial boundary layers, *Geomorphology* **68**, 1-2, 77-94, DOI: 10.1016/j.geomorph.2004. 09.032.

Byrd, T.C., D.J. Furbish, and J. Warburton (2000), Estimating depth-averaged velocities in rough channels, *Earth Surf. Process. Land.* **25**, 2, 167-173, DOI: 10.1002/(SICI)1096-9837(200002)25:2 <167::AID-ESP66> 3.0.CO;2-G.

Cardoso, A.H., W.H. Graf, and G. Gust (1989), Uniform flow in a smooth open channel, *J. Hydraul. Res.* **27**, 5, 603-616, DOI: 10.1080/ 00221688909499113.

Coceal, O., T.G. Thomas, I.P. Castro, and S.E. Belcher (2006), Mean flow and turbulence statistics over groups of urban-like cubical obstacles, *Bound.-Lay. Meteorol.* **121**, 3, 491-519, DOI: 10.1007/s10546-006-9076-2.

Coles, D. (1956), The law of the wake in the turbulent boundary layer, *J. Fluid Mech.* **1**, 2, 191-226, DOI: 10.1017/S0022112056000135.

Cooper, J.R., and S.J. Tait (2008), The spatial organisation of time-averaged streamwise velocity and its correlation with the surface topography of water-worked gravel beds, *Acta Geophys.* **56**, 3, 614-642, DOI: 10.2478/ s11600-008-0023-0.

da Franca, M.J.R.P. (2005), A field study of turbulent flows in shallow gravel-bed rivers, Ph.D. Thesis, École Polytechnique Fédérale De Lausanne, Lausanne, Switzerland.

Dong, Z.N., and Y. Ding (1990), Turbulence characteristics in smooth open-channel flow, *Sci. Chi. A* **33**, 2, 244-256.

Dong, Z.N., J.J. Wang, C.Z. Chen, and Z.H. Xia (1992), Hydraulic characteristics of open channel flows over rough beds, *Sci. Chi. A* **35**, 8, 1007-1016.

Einstein, H.A., and E.A. El-Samni (1949), Hydrodynamic forces on a rough wall, *Rev. Modern Phys.* **21**, 3, 520-524, DOI: 10.1103/RevModPhys.21.520.

Ferguson, R. (2007), Flow resistance equations for gravel- and boulder-bed streams, *Water Resour. Res.* **43**, 5, W05427, DOI: 10.1029/2006WR005422.

Ferro, V. (2003a), ADV measurements of velocity distributions in a gravel-bed flume, *Earth Surf. Process. Land.* **28**, 7, 707-722, DOI: 10.1002/esp.467.

Ferro, V. (2003b), Flow resistance in gravel-bed channels with large-scale roughness, *Earth Surf. Process. Land.* **28**, 12, 1325-1339, DOI: 10.1002/ esp.589.

Ferro, V., and G. Baiamonte (1994), Flow velocity profiles in gravel-bed rivers, *J. Hydraul. Eng. ASCE* **120**, 1, 60-80, DOI: 10.1061/(ASCE)0733-9429 (1994)120:1(60).

Hardy, R.J., J.L. Best, S.N. Lane, and P.E. Carbonneau (2009), Coherent flow structures in a depth-limited flow over a gravel surface: The role of near-bed turbulence and influence of Reynolds number, *J. Geophys. Res.* **114**, F01003, DOI: 10.1029/2007JF000970.

He, J.J., and H.M. Wang (2004), Hydraulic characteristics of open channel flow over a rough bed, *Hydro-Sci. Eng.* **3**, 3, 19-23 (in Chinese).

Jiménez, J. (2004), Turbulent flows over rough walls, *Ann. Rev. Fluid Mech.* **36**, 173-196, DOI: 10.1146/annurev.fluid.36.050802.122103.

Kastner-Klein, P., and M.W. Rotach (2004), Mean flow and turbulence characteristics in an urban roughness sublayer, *Bound.-Lay. Meteorol.* **111**, 1, 55-84, DOI: 10.1023/B:BOUN.0000010994.32240.b1.

Katul, G., P. Wiberg, J. Albertson, and G. Hornberger (2002), A mixing layer theory for flow resistance in shallow streams, *Water Resour. Res.* **38**, 11, DOI: 10.1029/2001WR000817.

Kim, S.C., C.T. Fredrichs, J.P.Y. Maa, and L.D. Wright (2000), Estimating bottom stress in tidal boundary layer from Acoustic Doppler Velocimeter data, *J. Hydraul. Eng. ASCE* **126**, 6, 399-406, DOI: 10.1061/(ASCE)0733-9429(2000)126:6(399).

Kirkgöz, M.S. (1989), Turbulent velocity profiles for smooth and rough open channel flow, *J. Hydraul. Eng. ASCE* **115**, 11, 1543-1561, DOI: 10.1061/(ASCE)0733-9429(1989)115:11 (1543).

Kirkgöz, M.S., and M. Ardiçlioğlu (1997), Velocity profiles of developing and developed open channel flow, *J. Hydraul. Eng. ASCE* **123**, 12, 1099-1105, DOI: 10.1061/(ASCE)0733-9429(1997)123:12(1099).

Knopp, T., T. Alrutz, and D. Schwamborn (2006), A grid and flow adaptive wall-function method for RANS turbulence modelling, *J. Comput. Phys.* **220**, 1, 19-40, DOI: 10.1016/j.jcp.2006.05.003.

Kuelegan, G.H. (1938), Laws of turbulent flow in open channels, Paper RP1181, *J. Res. Natl. Bur. Stand.* **21**, 701-741.

Lane, E.W., and E.J. Carlson (1953), Some factors affecting the stability of canals constructed in coarse granular materials. **In:** *Proc. Minnesota International Hydraulics Convention, 1-4 September 1953, Minneapolis, USA*, 37-48.

Legleiter, C.J., T.L. Phelps, and E.E. Wohl (2007), Geostatistical analysis of the effects of stage and roughness on reach-scale spatial patterns of velocity and turbulence intensity, *Geomorphology* **83**, 3-4, 322-345, DOI: 10.1016/j.geomorph.2006.02.022.

Lin, P., and C.W. Li (2002), A σ-coordinate three-dimensional numerical model for surface wave propagation, *Int. J. Numer. Meth. Fluids* **38**, 11, 1045-1068, DOI: 10.1002/fld.258.

Liu, C.J., D.X. Li, and X.K. Wang (2005), Experimental study on friction velocity and velocity profile of open channel flow, *J. Hydraul. Eng.* **36**, 8, 950-955 (in Chinese).

Marchand, J.P., R.D. Jarrett, and L.L. Jones (1984), Velocity profile, water-surface slope and bed-material size for selected streams in Colorado, Open-file Report 84-773, U.S. Geological Survey, Washington, USA.

Meyer-Peter, E., and R. Müller (1948), Formulas for bed-load transport. **In:** *Proc. 2nd Congress of the International Association for Hydraulic Research, Stockholm, Sweden*, 39-64.

Mignot, E., E. Barthélemy, and D. Hurther (2008), Turbulent kinetic energy budget in a gravel-bed channel flow, *Acta Geophys.* **56**, 3, 601-613, DOI: 10.2478/s11600-008-0020-3.

Mignot, E., D. Hurther, and E. Barthelemy (2009), On the structure of shear stress and turbulent kinetic energy flux across the roughness layer of a gravel-bed channel flow, *J. Fluid Mech.* **638**, 423-452, DOI: 10.1017/S0022112009990772.

Nepf, H., and M. Ghisalberti (2008), Flow and transport in channels with submerged vegetation, *Acta Geophys.* **56**, 3, 753-777, DOI: 10.2478/s11600-008-0017-y.

Nezu, I., and W. Rodi (1986), Open-channel flow measurements with a Laser Doppler Anemometer, *J. Hydraul. Eng. ASCE* **112**, 5, 335-355, DOI: 10.1061/(ASCE)0733-9429(1986)112:5(335).

Nikora, V.I., and D.G. Goring (1998), ADV measurements of turbulence: Can we improve their interpretation? *J. Hydraul. Eng. ASCE* **124**, 6, 630-634, DOI: 10.1061/(ASCE)0733-9429(1998)124:6(630).

Nikora, V.I., I. McEwan, S. McLean, S. Coleman, D. Pokrajac, and R. Walters (2007), Double-averaging concept for rough-bed open-channel and overland flows: Theoretical background, *J. Hydraul. Eng.* **133**, 8, 873-883, DOI: 10.1061/(ASCE)0733-9429(2007)133:8(873).

Nowell, A.R.M., and M. Church (1979), Turbulent flow in a depth-limited boundary layer, *J. Geophys. Res:* **84**, C8, 4816-4824, DOI: 10.1029/JC084iC08p04816.

Papanicolaou, A.N., C.M. Kramer, A.G. Tsakiris, T. Stoesser, S. Bomminayuni, and Z. Chen (2012), Effects of a fully submerged boulder within a boulder array on the mean and turbulent flow fields: Implications to bedload transport, *Acta Geophys.* **60**, 6, 1502-1546, DOI: 10.2478/s11600-012-0044-6.

Raupach, M.R. (1981), Conditional statistics of Reynolds stress in rough-wall and smooth-wall turbulent boundary layers, *J. Fluid Mech.* **108**, 363-382, DOI: 10.1017/S0022112081002164.

Raupach, M.R., J.J. Finnigan, and Y. Brunet (1996), Coherent eddies and turbulence in vegetation canopies: the mixing-layer analogy, *Bound.-Lay. Meteorol.* **78**, 3-4, 351-382, DOI: 10.1007/BF00120941.

Robert, A., A.G. Roy, and B. de Serres (1992), Changes in velocity profiles at roughness transitions in coarse grained channels, *Sedimentology* **39**, 5, 725-735, DOI: 10.1111/j.1365-3091.1992.tb02149.x.

Rowiński, P.M., J. Aberle, and A. Mazurczyk (2005), Shear velocity estimation in hydraulic research, *Acta Geophys. Pol.* **53**, 4, 567-583.

Roy, A.G., T. Buffin-Bélanger, H. Lamarre, and A.D. Kirkbride (2004), Size, shape and dynamics of large-scale turbulent flow structures in a gravel-bed river, *J. Fluid Mech.* **500**, 1-27, DOI: 10.1017/S0022112003006396.

Schindler, R.J., and A. Robert (2005), Flow and turbulence structure across the rip-ple-dune transition: an experiment under mobile bed conditions, *Sedimen-tology* **52**, 3, 627-649, DOI: 10.1111/j.1365-3091.2005.00706.x.

Schmeeckle, M.W., and J.M. Nelson (2003), Direct numerical simulation of bedload transport using a local, dynamic boundary condition, *Sedimentology* **50**, 2, 279-301, DOI: 10.1046/j.1365-3091.2003.00555.x.

Shvidchenko, A.B., and G. Pender (2001), Macroturbulent structure of open-channel flow over gravel beds, *Water Resour. Res.* **37**, 3, 709-719, DOI: 10.1029/2000WR900280.

Singh, A., F. Porté-Agel, and E. Foufoula-Georgiou (2010), On the influence of gravel bed dynamics on velocity power spectra, *Water Resour. Res.* **46**, 4, W04509, DOI: 10.1029/2009WR008190.

Stoesser, T., and V.I. Nikora (2008), Flow structure over square bars at intermediate submergence: Large Eddy Simulation study of bar spacing effect, *Acta Geophys.* **56**, 3, 876-893, DOI: 10.2478/s11600-008-0030-1.

Tachie, M.F., D.J. Bergstrom, and R. Balachandar (2000), Rough wall turbulent boundary layers in shallow open channel flow, *J. Fluids Eng.* **122**, 3, 533-541, DOI: 10.1115/1.1287267.

Wang, D.C., X.K. Wang, and D.X. Li (1998), Mean velocity distributions and im-pact factor analysis of open channel flows, *J. Sediment. Res.* **3**, 86-90 (in Chinese).

Wang, X.Y., X.K. Wang, X.N. Liu, W.Z. Lu, and Q.Y. Yang (2007), Calculation methods of shear velocity in open gravel channel, *Adv. Sci. Technol. Water Res.* **27**, 5, 14-18 (in Chinese).

Wohl, E.E., and H. Ikeda (1998), The effect of roughness configuration on velocity profiles in an artificial channel, *Earth Surf. Process. Land.* **23**, 2, 159-169, DOI: 10.1002/(SICI)1096-9837(199802)23:2<159::AID-ESP829>3.0.CO; 2-P.

Wohl, E.E., and D.M. Thompson (2000), Velocity characteristics along a small step-pool channel, *Earth Surf. Process. Land.* **25**, 4, 353-367, DOI: 10.1002/(SICI)1096-9837(200004)25:4 <353::AID-ESP59>3.0.CO;2-5.

Yang, B., and S.F. Yang (2005), The experimental study on the velocity distribution over the high gradient gravel bed, *J. Hydrodyn.* **20**, 2, 207-213 (in Chinese).

Zippe, H.J., and W.H. Graf (1983), Turbulent boundary-layer flow over permeable and non-permeable rough surfaces, *J. Hydrol. Res.* **21**, 1, 51-65, DOI: 10.1080/00221688309499450.